Chinese Journal of Natural Medicines

Carrimycin ameliorates lipopolysaccharide and cecal ligation and puncture-induced sepsis in mice

Junzhong LAI, Jiadi LIANG, Kunsen CHEN, Biyun GUAN, Zhirong CHEN, Linqin CHEN, Jiqiang FAN, Yong ZHANG, Qiumei LI, Jingqian SU, Qi CHEN, Jizhen LIN

Citation: Junzhong LAI, Jiadi LIANG, Kunsen CHEN, Biyun GUAN, Zhirong CHEN, Linqin CHEN, Jiqiang FAN, Yong ZHANG, Qiumei LI, Jingqian SU, Qi CHEN, Jizhen LIN, Carrimycin ameliorates lipopolysaccharide and cecal ligation and puncture-induced sepsis in mice, Chinese Journal of Natural Medicines, 2024, 22(3), 235-248. doi: 10.1016/S1875-5364(24)60600-X.

View online: https://doi.org/10.1016/S1875-5364(24)60600-X

Available online at www.sciencedirect.com
ScienceDirect
Chinese Journal of Natural Medicines 2024, **22**(3): 235-248
doi: 10.1016/S1875-5364(24)60600-X
Chinese Journal of Natural Medicines

•Original article•

Carrimycin ameliorates lipopolysaccharide and cecal ligation and puncture-induced sepsis in mice

LAI Junzhong[1Δ], LIANG Jiadi[1, 2Δ], CHEN Kunsen[2], GUAN Biyun[2], CHEN Zhirong[2], CHEN Linqin[2], FAN Jiqiang[2], ZHANG Yong[2], LI Qiumei[2], SU Jingqian[2], CHEN Qi[2*], LIN Jizhen[1, 3*]

[1] *The Cancer Center, Fujian Medical University Union Hospital, Fuzhou 350001, China;*
[2] *Fujian Key Laboratory of Innate Immune Biology, Biomedical Research Center of South China, Fujian Normal University, Fuzhou 350117, China;*
[3] *The Department of Otolaryngology, Head & Neck Surgery, University of Minnesota Medical School, Minneapolis, MN 55455, USA*

Available online 20 Mar., 2024

[ABSTRACT] Carrimycin (CA), sanctioned by China's National Medical Products Administration (NMPA) in 2019 for treating acute bronchitis and sinusitis, has recently been observed to exhibit multifaceted biological activities, encompassing anti-inflammatory, antiviral, and anti-tumor properties. Despite these applications, its efficacy in sepsis treatment remains unexplored. This study introduces a novel function of CA, demonstrating its capacity to mitigate sepsis induced by lipopolysaccharide (LPS) and cecal ligation and puncture (CLP) in mice models. Our research employed *in vitro* assays, real-time quantitative polymerase chain reaction (RT-qPCR), and RNA-seq analysis to establish that CA significantly reduces the levels of pro-inflammatory cytokines, namely tumor necrosis factor-alpha (TNF-α), interleukin 1 beta (IL-1β), and interleukin 6 (IL-6), in response to LPS stimulation. Additionally, Western blotting and immunofluorescence assays revealed that CA impedes Nuclear Factor Kappa B (NF-*κ*B) activation in LPS-stimulated RAW264.7 cells. Complementing these findings, *in vivo* experiments demonstrated that CA effectively alleviates LPS- and CLP-triggered organ inflammation in C57BL/6 mice. Further insights were gained through 16S sequencing, highlighting CA's pivotal role in enhancing gut microbiota diversity and modulating metabolic pathways, particularly by augmenting the production of short-chain fatty acids in mice subjected to CLP. Notably, a comparative analysis revealed that CA's anti-inflammatory efficacy surpasses that of equivalent doses of aspirin (ASP) and TIENAM. Collectively, these findings suggest that CA exhibits significant therapeutic potential in sepsis treatment. This discovery provides a foundational theoretical basis for the clinical application of CA in sepsis management.

[KEY WORDS] Carrimycin; Inflammation; Lipopolysaccharide; Cecal ligation and puncture; Sepsis; Gut microbiota
[CLC Number] R965 **[Document code]** A **[Article ID]** 2095-6975(2024)03-0235-14

Introduction

Sepsis, a systemic inflammatory response syndrome instigated by pathogen infection, is accompanied by immune dysregulation and represents a significant challenge in modern intensive care [1]. This condition is characterized by high morbidity and mortality rates and can lead to multiple sequelae, including cognitive impairment [2] and chronic diseases [3]. Research has identified the primary causes of immune disorders in sepsis as excessive activation of the complement system [4], coagulation system [5], vascular endothelial cells [6], and alterations in the function and programming of antigen-presenting cells [7, 8]. Moreover, patients with sepsis face ongoing challenges due to the relentless invasion of pathogenic microorganisms, predominantly gram-positive bacteria like Staphylococcus aureus and Streptococcus pneumoniae, and gram-negative bacteria such as *Escherichia coli*, *Klebsiella*, and *Pseudomonas aeruginosa* [9].

Upon pathogen invasion, the body employs pattern recognition receptors (PRRs) to detect pathogen-associated molecular patterns (PAMPs), subsequently activating canonical and non-canonical Nuclear Factor Kappa B (NF-*κ*B) pathways through toll-like receptors (TLRs). Persistent pathogen presence leads to continuous immune activation, potentially

[Received on] 14-Jul.-2023
[Research funding] This work was supported by the Excellent Young Scholars Cultivation Project of Fujian Medical University Union Hospital in China (No. 2022XH031), the National Natural Science Foundation of China (No. 82203439), and the Natural Science Foundation of Fujian Province (No. 2022J01263).
[*Corresponding author] E-mails: chenqi@fjnu.edu.cn (CHEN Qi); linjizhen@fjmu.edu.cn (LIN Jizhen)
ΔThese authors contributed equally to this work.
These authors have no conflict of interest to declare.

resulting in prolonged and life-threatening immune dysregulation. Consequently, the prompt removal of pathogenic microorganisms is crucial. Fluid purification is a recognized therapeutic approach to control sepsis progression [10, 11]; however, determining the optimal dosage, rate, and composition of intravenous infusions to enhance treatment efficacy in sepsis patients requires further research [12].

In the realm of sepsis treatment, various immunomodulators, including cytokines, transcription factors, and coagulation activators, have been evaluated [13]. While these have shown promise in preclinical studies, their efficacy in clinical trials remains to be validated. Given the complex pathophysiology of sepsis, immunomodulators with singular functions and targets may prove inadequate. Their potential use in combination therapies is an area of interest but also requires substantiation. Additionally, international guidelines strongly recommend antibacterial therapy in the early stages of sepsis [14]. *β*-Lactam treatments have been beneficial in alleviating sepsis symptoms and reducing mortality in clinical settings [15, 16]. However, treatments targeting the immune and metabolic abnormalities induced by sepsis are still under development and require further investigation.

Carrimycin (CA), also known as bitespiramycin and shengjimycin, is a 16-membered macrolide antibiotic comprising primarily isovalerylspiramycin (ISP) components I, II, and III. This antibiotic is produced by genetically engineered spiramycin-producing bacteria [17]. Approved by China's National Medical Products Administration (NMPA) in 2019 for treating acute bronchitis and sinusitis, CA's safety and exceptional antibacterial properties have been well-established in numerous studies [18-20].

In vitro, CA has demonstrated superior antibacterial efficacy compared with acetylspiramycin, and its effectiveness is comparable to azithromycin. It is particularly effective against pathogens such as *Chlamydia trachomatis*, *Chlamydia pneumoniae*, *Ureaplasma urealyticum*, and *Mycoplasma pneumoniae* [21], which are known to be associated with sepsis arising from pelvic infections [22], pulmonary infection [23], and childbirth infection [24]. In addition to its antibacterial properties, recent studies have unveiled CA's potential as an antiviral and anti-tumor agent. During the COVID-19 pandemic, CA emerged as a candidate for combating human coronavirus infection, and its efficacy is currently being evaluated in clinical trials [25]. Furthermore, CA has been shown to modulate the PI3K/AKT/mTOR and mitogen-activated protein kinase (MAPK) pathways, influencing the cell cycle and promoting apoptosis in human oral squamous cell carcinoma cells [26]. Both CA and monomeric ISP I have been found to impact the expression of vascular endothelial growth factor and programmed death-ligand 1 (PD-L1), thereby inhibiting the proliferation, migration, and invasion of hepatoma cells [27]. Additionally, ISP I can disrupt ribosomal RNA transcription by inhibiting the nucleolar protein selenoprotein H, leading to reactive oxygen species (ROS) accumulation and triggering the JNK2/TIF-IA/POLI pathway. This pathway induces cell cycle arrest and apoptosis in cancer cells [28]. These findings highlight CA's considerable potential for further functional development, extending beyond its role as an antibiotic.

Data from Shenyang Tonglian Group indicate that CA possesses antibacterial activity against *β*-lactam resistant bacteria, such as Streptococcus pneumoniae and Staphylococcus aureus. A clinical study has also reported that azithromycin treatment correlates with a lower incidence of acute kidney injury in sepsis [29]. Notably, while CA's antibacterial activity *in vitro* is comparable to that of azithromycin, CA has demonstrated superior efficacy over azithromycin *in vivo* in hamster experiments with Mycoplasma pneumoniae infections [21]. Furthermore, CA has received approval from the NMPA for treating acute bronchitis, a significant condition considering respiratory failure since pneumonia is a leading cause of death in sepsis patients. These aspects underscore the potential of CA's antibacterial and anti-inflammatory properties in treating sepsis.

In our study, we explored the viability of CA in treating sepsis induced by lipopolysaccharide (LPS) and cecal ligation and puncture (CLP) in mice, assessing both the safety of CA and its effectiveness in inflammation inhibition, both *in vivo* and *in vitro*. Additionally, we investigated the impact of CA on the gut microbiota composition in CLP mice. Our findings demonstrated that CA exhibits remarkable anti-inflammatory properties, primarily by hindering NF-*κ*B-mediated (nuclear factor kappa B) immune activation and by modulating gut microbiota diversity. Based on these results, CA emerges as a promising therapeutic agent for sepsis treatment.

Material and Methods

Compounds

Carrimycin was sourced from Shenyang Tonglian Group Co., Ltd. (Shenyang, China). ISP I and ISP III were isolated and purified from Carrimycin, but due to a complex separation process, ISP II could not be extracted. For clarity, in this study, carrimycin was referred to as CA, ISP I as CA01, and ISP III as CA03.

Cell culture and LPS stimulation

Mouse macrophage cell lines RAW264.7 and RAW-Lucia™ ISG were acquired from InvivoGen (California, USA) and maintained in a medium supplemented with 10% (*V*/*V*) fetal bovine serum (FBS) (Gibco, Grand Island, USA) and 1% (*V*/*V*) penicillin-streptomycin (BesalMedia, Shanghai, China). The cells were cultured at 37 °C in a humidified incubator with 5% CO2. THP1 (Tohoku Hospital Pediatrics-1) cells (InvivoGen, California, USA) were cultured under similar conditions, except the FBS was heat-inactivated (56 °C for 30 min).

The RAW264.7, RAW-Lucia™ ISG, and THP1 cells were utilized to investigate the *in vitro* anti-inflammatory effects of CA. Cells were pre-treated with CA, followed by LPS (Cell Signaling Technology, Boston, USA) stimulation to induce inflammation.

Cell cytotoxicity assay

To assess CA's cytotoxicity, the Cell Counting Kit-8 (CCK-8) from MedChemExpress (New Jersey, USA) was used. Cells were seeded in 96-well plates and treated with varying concentrations of CA for 24 h. Afterward, CCK-8 solution was added to each well and incubated at 37 °C for 2 h. The optical density (OD) at 450 nm was measured to evaluate cell viability.

Real-time quantitative polymerase chain reaction (RT-qPCR) assay

The RT-qPCR assay was employed to quantify the mRNA expression changes induced by CA treatment in LPS-stimulated cells. Total RNA was extracted using TRIzol (Takara, Shiga Prefecture, Japan) and reverse transcribed using a cDNA synthesis kit (Yeasen, Shanghai, China). The RT-qPCR was conducted using SYBR Green Mix (Yeasen, Shanghai, China) on a QuantStudio 6 Flex system (Thermo, Massachusetts, USA). The primers used for amplifying the target genes are detailed in Tables S1 and S2.

Western blotting analysis

For protein extraction, Radioimmunoprecipitation assay (RIPA) buffer (Beyotime, China) was utilized, and protein concentrations were ascertained using the BCA protein assay kit (Beyotime, Jiangsu, China). Equal quantities of protein were separated by sodium dodecyl sulfate–polyacrylamide gel electrophoresis (SDS-PAGE) and subsequently transferred onto methanol-activated Polyvinylidene Fluoride (PVDF) membranes. The membranes were then blocked using Immobilon Signal Enhancer (Sigma-Aldrich, Missouri, USA) for 1 hour and incubated overnight at 4 °C with specific primary antibodies. Following three washes, the membranes were incubated with appropriate secondary antibodies and visualized using the Infrared Molecular Imaging System Odyssey C1 (Gene Company Limited, Hong Kong, China). Protein markers and antibodies used in this study are as follows: Pre-stained Protein Marker 10-180 KD (P1018, Beijing Lablead Biotech, China). Anti-NF-*κ*B mouse monoclonal antibody (mAb) (6956, Cell Signaling Technology, Boston, USA). Anti-phospho-NF-*κ*B mouse mAb (13346, Cell Signaling Technology, Boston, USA). Anti-IκBα rabbit polyclonal antibody (pAb) (A16929, ABclonal Technology, Wuhan, China). Anti-phospho-I*κ*B*α* (inhibitor of nuclear factor kappa B) rabbit mAb (AP0707, ABclonal Technology, Wuhan, China). Anti-GAPDH (Glyceraldehyde 3-phosphate dehydrogenase) mouse mAb (97166, Cell Signaling Technology, Boston, USA). Anti-PI3K (Phosphoinositide 3-kinase) rabbit pAb (20584-1-AP, Proteintech, Wuhan, China). Anti-phospho-PI3K rabbit mAb (17366S, Cell Signaling Technology, Boston, USA). Anti-AKT mouse mAb (60203-2-Ig, Proteintech, Wuhan, China). Anti-phospho-AKT mouse mAb (66444-1-Ig, Proteintech, Wuhan, China). IRDye® 800CW Donkey Anti-Mouse IgG Secondary Antibody (925-32212, LICOR, USA). RDye® 800CW Donkey Anti-Rabbit IgG Secondary Antibody (926-32213, LICOR, USA).

Immunofluorescence

Cells were cultured in glass bottom dishes (NEST Biotechnology Co., Ltd., Wuxi, China) and maintained at 37 °C in a humidified atmosphere containing 5% CO_2. Following treatment with CA and LPS, the cells underwent a fixation process using 4% paraformaldehyde for 10 m. They were then permeabilized with Triton-X100 (Beyotime, Jiangsu, China) for 15 min. To minimize non-specific binding, cells were blocked with 5% BSA for 1 h. This was followed by overnight incubation at 4 °C with primary antibodies against NF-*κ*B (6956, Cell Signaling Technology, Boston, USA) and I*κ*B-α (A16929, ABclonal Technology, Wuhan, China), diluted at 1 ∶ 200. Subsequent to the primary antibody incubation, cells were treated with Alexa Fluor 594 goat anti-mouse secondary antibody (Thermo, Massachusetts, USA) at a 1 ∶ 1000 dilution for 1 h. For nuclear staining, DAPI (Thermo, Massachusetts, USA) was applied for 2 min. The stained cells were visualized under a Zeiss fluorescence microscope (using a 100× objective lens, LSM780, Carl Zeiss, Oberkochen, Germany). The acquired images were analyzed using Zeiss LSM 510 software. This comprehensive approach provides a detailed visualization of the cellular responses to CA and LPS, particularly focusing on the localization and expression of NF-*κ*B and I*κ*B-α, thus offering valuable insights into the molecular mechanisms of CA's action.

Mouse study

C57BL/6 mice were procured from Shanghai Wushi Animals (China) and housed at the Animal Center of Fujian Normal University. The facility provided an SPF (Specific Pathogen Free) environment with 50% humidity and a maintained temperature of 24 ± 1 °C. The mice were subjected to a 12-h light/dark cycle and had unrestricted access to food and water. All experimental procedures involving animals were conducted in strict accordance with the Guideline for the Care and Use of Laboratory Animals. These procedures received approval from the Animal Care and Use Committee of Fujian Normal University. The specific animal study protocol was sanctioned by the Animal Ethical and Welfare Committee of Fujian Normal University under the protocol code IACUC-20210022, approved on March 16, 2021.

Male and female mice, aged 8–10 weeks and weighing approximately 20 ± 1 g, were randomly divided into four groups: control, CA, sepsis, and CA plus sepsis. CA was dissolved in a solvent consisting of 80% corn oil and 20% polyethylene glycol 400 to prepare the CA solution. Oral gavage was performed once daily for three days at a dosage of 100 $mg \cdot kg^{-1}$ of CA per mouse, while the control group received an equivalent amount of the solvent.

To study the therapeutic effect of CA on sepsis, LPS- and CLP-induced sepsis mouse models were generated on day 4. For the LPS model, mice were intraperitoneally injected with 15 $mg \cdot kg^{-1}$ LPS (CST, Boston, USA), dissolved in saline, to induce sepsis. The control group received an equivalent volume of normal saline.

The CLP model involved anesthetizing the mice with tribromoethanol (Sigma-Aldrich, Missouri, USA), followed

by shaving and sterilizing the abdominal hair. A laparotomy exposed the cecum, which was then ligated with sutures and punctured using an 18G needle. The cecal contents were gently extruded, and the cecum was returned to the abdominal cavity along with the extruded contents before suturing the layers back together [30]. Each mouse then received a subcutaneous injection of 1 mL of normal saline for resuscitation. The control group underwent a sham surgery identical to the CLP procedure, except for the cecal puncture.

Histopathological examination

This comprehensive experimental setup is crucial for evaluating the potential therapeutic effects of Carrimycin in sepsis treatment, using well-established animal models to simulate the condition.

Enzyme-linked immunosorbent assay (ELISA)

For quantifying the levels of interleukin 6 (IL-6) and interleukin 1 beta (IL-1β), as well as tumor necrosis factor-alpha (TNF-α) in the peripheral blood of mice, serum samples were collected and analyzed using ELISA kits from Invitrogen (California, USA). The assays were performed strictly in accordance with the manufacturer's provided protocol.

Sequencing

The total RNA from RAW264.7 cells was extracted and subsequently dispatched to Novogene (Beijing, China) for RNA sequencing (RNA-seq). Additionally, intestinal fecal samples from CLP mice were collected and sent to Biomarker Technologies (BMK, Beijing, China) for 16S ribosomal RNA sequencing (16SrRNA-seq).

Statistical analysis

All experimental data are expressed as mean ± standard error of the mean (SEM). To ensure reliability, each experiment was conducted at least three times independently. The statistical analysis between groups was performed using Student's *t*-test, facilitated by GraphPad software. A *P*-value of less than 0.05 was considered indicative of statistical significance. The specific level of significance for each comparison is denoted in the figure legends as follows: ns (no significance), $^{*}P < 0.05$, $^{**}P < 0.01$, $^{***}P < 0.001$, $^{****}P < 0.0001$.

Results

Carrimycin potently inhibits LPS-induced inflammation

CA, a multi-component drug, primarily comprises ISP I (CA01), ISP II, and ISP III (CA03) as its main constituents [17, 20] (Fig. 1A). Given that persistent inflammation is a critical factor leading to organ damage and can be life-threatening in sepsis patients [31], controlling inflammation is of paramount importance. Our study initially focused on cellular-level investigations to assess CA's anti-inflammatory properties.

The cytotoxic effects of CA, CA01, and CA03 at various concentrations were evaluated using the CCK8 cell viability assay (Figs. S1A–1C). Results indicated no cytotoxicity at concentrations up to 10 μg·mL^{-1}. We assessed the influence of these compounds on LPS-induced interferon-beta (IFN-β) production using luciferase assays in RAW-Lucia™ ISG cells (Figs. S2A–2C). The findings revealed that while none of the compounds exerted significant cytotoxic effects, they all inhibited LPS-induced IFN-β expression. Comparing the effects of 10 μg·mL^{-1} CA, CA01, and CA03 on LPS-induced cytokine production, it was observed that CA was more effective in inhibiting the mRNA expression levels of IL-6, IL-1β, and TNF-α compared with CA01 and CA03 (Figs. 1B–1D). Consequently, CA was selected for subsequent experiments. Similar inhibitory effects on IL-6, IL-1β, and TNF-α mRNA expression levels in THP1 cells were observed with 10 μg·mL^{-1} CA (Figs. S3A–S3C). Furthermore, CA also reduced the protein expression levels of these cytokines in RAW264.7 cells (Figs. 1E–1G). These findings collectively indicate that CA effectively counters LPS-induced inflammatory responses in RAW264.7 and THP1 cells.

RNA sequencing was conducted to examine the differential gene expression following treatment with 10 μg·mL^{-1} CA in the context of LPS-induced inflammation. The data suggested that CA's mitigation of LPS-induced inflammation is linked to changes in several immune activation signaling pathways, including the NF-κB signaling pathway (Fig. 1I). Specifically, CA reduced the expression of IL-6, IL-1β, NF-κB1, and other related genes that were upregulated by LPS (Fig. 1J). These findings were further corroborated by RT-qPCR analyses (Figs. S4A–4L).

Carrimycin impairs immune activation of NF-κB in vitro

Given that CA effectively downregulated mRNA expression of NF-κB in response to LPS stimulation, further investigations were conducted to evaluate its influence on related protein expression within the NF-κB signaling pathway. LPS is known to activate the IKK complex, leading to the phosphorylation of IκB. This phosphorylation event facilitates the release of the NF-κB complex, thereby triggering an inflammatory response [32]. Fig. 2C illustrates that CA inhibited the protein expression of phosphorylated IκB-α (p-IκB-α) and phosphorylated NF-κB (p-NF-κB) induced by LPS. These results indicate a direct impact of CA on the key regulatory proteins in the NF-κB pathway, which is central to the inflammatory response. Corroborating the findings from Western blotting analysis, immunofluorescence assays revealed that CA diminished the LPS-induced reduction of IκB-α (Fig. 2A) and impeded the nuclear entry of NF-κB (Fig. 2B). These observations provide visual evidence of CA's ability to modulate key steps in the NF-κB pathway, specifically the stabilization of IκB-α and the nuclear translocation of NF-κB. Additionally, the role of the PI3K/AKT pathway, an upstream regulator of NF-κB, was examined through Western blotting analysis. However, in LPS-induced RAW264.7 cells, CA did not exhibit a significant effect on the protein expression levels of the PI3K/AKT pathway (Fig. S5). This finding suggests that CA's anti-inflammatory action is likely confined to the modulation of the NF-κB pathway rather than involving upstream signaling pathways like PI3K/AKT. These results collectively suggest that Carrimycin can attenuate LPS-induced inflammation primarily by regulating the NF-κB sig-

naling pathway *in vitro*. This targeted modulation presents CA as a potential therapeutic agent in managing inflammation, particularly in conditions like sepsis where NF-*κ*B-mediated pathways play a critical role.

Carrimycin exhibits low toxicity in vivo

To evaluate the *in vivo* effect of CA, we initially investigated its toxicity in C57BL/6 mice. The study involved administering various concentrations of CA (ranging from 25 to 200 mg·kg^{-1}·d^{-1}) to the mice for 6 d to understand CA's pharmacokinetic profile. The findings indicated no significant impact on the body weight of the mice at the conclusion of the dosage period (Fig. 3A). Subsequently, an array of mouse organs, including the heart, liver, spleen, lung, and kidney, were examined post-treatment. The results showed that CA did not notably influence the weight of these organs (Fig. 3B). Additionally, histopathological analysis *via* Hematoxylin and Eosin (H&E) staining revealed no evident toxicity or adverse effects of CA (within the concentration range of 25–200 mg·kg^{-1}·d^{-1}) on the lung and liver tissues of the mice (Figs. 3C–3D). Moreover, RT-qPCR analysis demonstrated that CA exerted a dose-dependent inhibitory effect on the expression of LPS-induced pro-inflammatory cytokines such as IL-6, IL-1β, and TNF-α in mouse lung tissue. A concentration of 100 mg·kg^{-1} was determined to be the optimal dose, as its efficacy was not significantly different from that of 200 mg·kg^{-1}, as evidenced by Figs. S6A–6C. These findings collectively suggest that CA, within the tested concentration range, is not associated with evident toxicity in C57BL/6 mice and effectively inhibits pro-inflammatory cytokine production in lung tissue, indicating its potential therapeutic efficacy in treating conditions like sepsis.

Carrimycin effectively relieves LPS-induced sepsis in mice

The therapeutic efficacy of CA on LPS-induced inflammation was rigorously assessed in this study. Mice were administered CA (100 mg·kg^{-1}) three times *via* gavage, which was found to mitigate the hypothermia induced by LPS (15 mg·kg^{-1}) (Figs. 4A–4B). Additionally, CA administration significantly enhanced the survival rate of LPS-treated mice (Fig. 4C). In the context of sepsis, prolonged inflammatory responses can precipitate organ damage and failure [33]. Our findings revealed that CA effectively reduced the mRNA expression levels of pro-inflammatory cytokines IL-6, IL-1β, and TNF-α in both the liver (Figs. 4D–4F) and lung (Figs. 4G–4I) of mice with LPS-induced sepsis. Histopathological analyses using H&E staining demonstrated that CA ameliorated lesions and decreased neutrophil infiltration in the lung

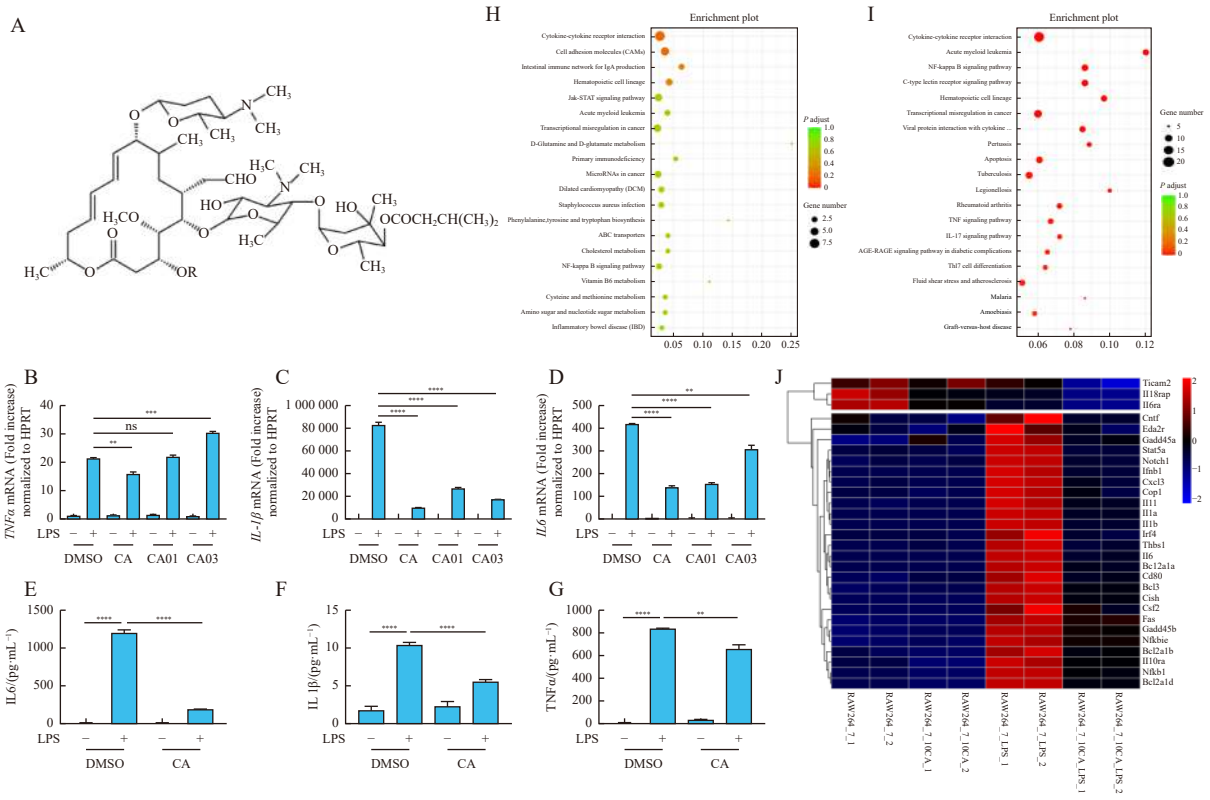

Fig. 1 Carrimycin inhibits LPS-induced expression of inflammatory factors in RAW264.7 cells. (A) Chemical structural formulas of CA and its major components, ISP I (R = H), ISP II (R = $COCH_3$), and ISP III (R = $COCH_2CH_3$). (B–D) mRNA expressions of IL-6, IL-1β, and TNF-α in cells, measured after 8 h of LPS (1 μg·mL^{-1}) stimulation (n = 3). (E–G) The levels of IL-6, IL-1β, and TNF-α in the cell culture medium, measured after 12 h of LPS (1 μg·mL^{-1}) stimulation (n = 3). (H–I) The top 20 signaling pathways in the KEGG enrichment analysis in mock *vs* CA (H) and LPS *vs* CA + LPS (I). (J) Heatmap showing differential expression of the 29 enriched genes across groups (Mock, CA, LPS, and CA + LPS). Data are represented as mean ± SEM. $^{**}P$ < 0.01, $^{***}P$ < 0.001, $^{****}P$ < 0.0001.

and liver tissues of these mice (Figs. S7A–7D). It is noteworthy that increased neutrophil infiltration is a known contributor to septic respiratory failure and liver damage [33, 34]. The organ-protective effects of CA in LPS-induced mice might be attributed to its favorable pharmacokinetic properties, including high tissue affinity and extended half-life [18]. Further evaluation of inflammatory markers in the mice's blood revealed a significant decrease in IL-6, IL-1β, and TNF-α levels in the peripheral blood of mice treated with CA following LPS induction (Figs. 4J–4L). Western blotting analysis corroborated these findings, showing that CA inhibited the expression of phosphorylated IκB-α and NF-κB in the lung tissue of mice (Fig. 4M). The inhibition of NF-κB signaling is known to reduce the expression of inflammatory factors. In summary, these data collectively underscore the potency of CA in alleviating systemic inflammation in LPS-induced sepsis in mice. This is evidenced by the reduction in systemic inflammatory responses, the mitigation of lung and liver tissue damage, and the inhibition of the NF-κB signaling pathway. These results provide substantial support for the potential application of CA as a therapeutic agent in sepsis treatment.

Carrimycin treats CLP-induced sepsis in mice

The CLP model is recognized as the "gold standard" in sepsis research [35], providing a highly relevant clinical scenario for studying sepsis-induced inflammation. In this context, we utilized the CLP model to validate the therapeutic effects of CA in sepsis.

Behavioral observations were the initial step in our experiment. Post-surgery, CLP mice exhibited notable symptoms consistent with sepsis, including reduced activity, curling up, trembling, and the secretion of white mucus from the orbit. These symptoms were markedly alleviated following the administration of CA (100 mg·kg^{-1}, administered *via* gavage three times, once every two days), as illustrated in Figs. 5A and 5M. The study further revealed that CA treatment significantly enhanced the survival rate of the CLP-induced mice (Fig. 5C). Moreover, CA helped in maintaining a stable body temperature in these mice (Fig. 5B). A critical aspect of the study was the evaluation of inflammatory markers. CA treatment notably decreased the mRNA expression levels of key inflammatory factors, including IL-6, IL-1β, and TNF-α, in both the liver (Figs. 5D–5F) and lung (Figs. 5G–5I) of CLP-induced mice. Corroborating these findings, a significant reduction in the serum levels of IL-6, IL-1β, and TNF-α was observed in the CA-treated CLP-induced mice (Figs. 5J–5L). In summary, these results strongly suggest that CA treatment exerts a beneficial therapeutic effect in reducing systemic inflammation in CLP-induced septic mice. This evidence underscores the potential of CA as a viable therapeutic agent in the treatment of sepsis, offering promising avenues for further clinical research and application.

Carrimycin influences the distribution of gut microbiota in CLP mice

The susceptibility to sepsis is closely linked to alterations in gut microbiota, with its pathogenesis involving the proliferation of intestinal pathogens, triggering immune-inflammatory responses, and a reduction in intestinal probiotic

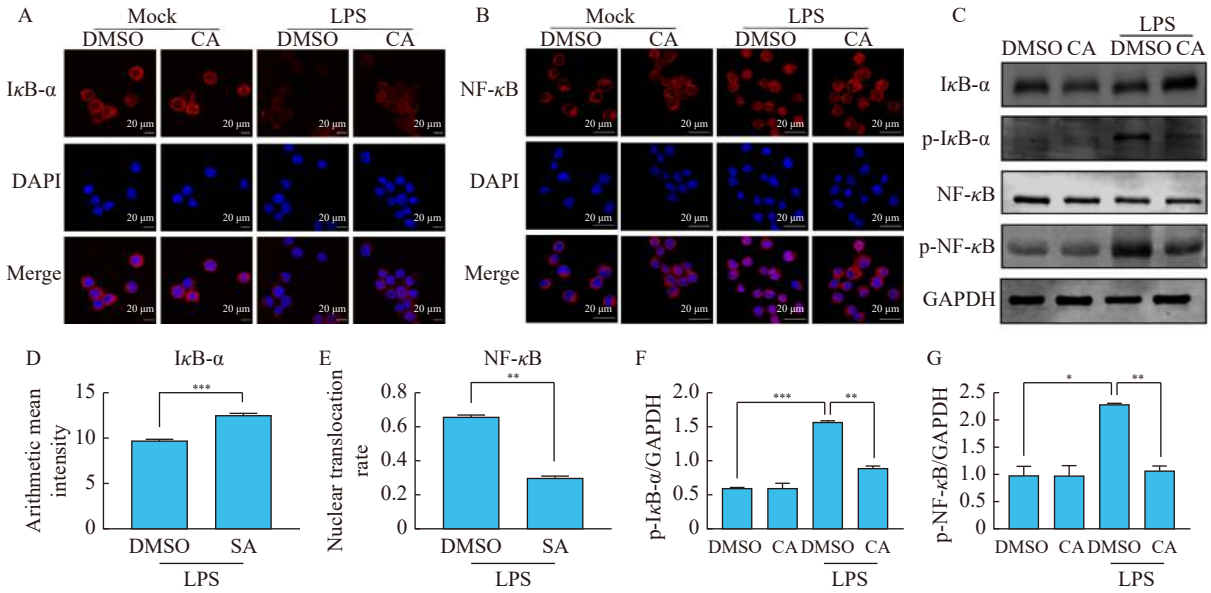

Fig. 2 Carrimycin affects LPS-induced inflammation by mediating the NF-κB pathway. (A–B) Immunofluorescence results show that 10 μg·mL^{-1} CA preserved the LPS-induced reduction of IκB-α (A) and decreased the NF-κB nuclear entry rate (B) when RAW264.7 cells were stimulated with LPS (1 μg·mL^{-1}) for 15 min. (C) Western blotting results show that 10 μg·mL^{-1} CA affected LPS-induced (1 μg·mL^{-1}) protein expression of the NF-κB signaling pathway. (D–E) The arithmetic mean intensity of IκB-α (D) and the rate of nuclear translocation of NF-κB (E) were quantified and plotted in immunofluorescence (A and B). (F–G) Protein levels of p-IκB-α (F) and p-NF-κB (G) were quantified and plotted in Western blotting assay (C). Data are represented as mean ± SEM (n = 3). $^{*}P < 0.05$, $^{**}P < 0.01$, $^{***}P < 0.001$.

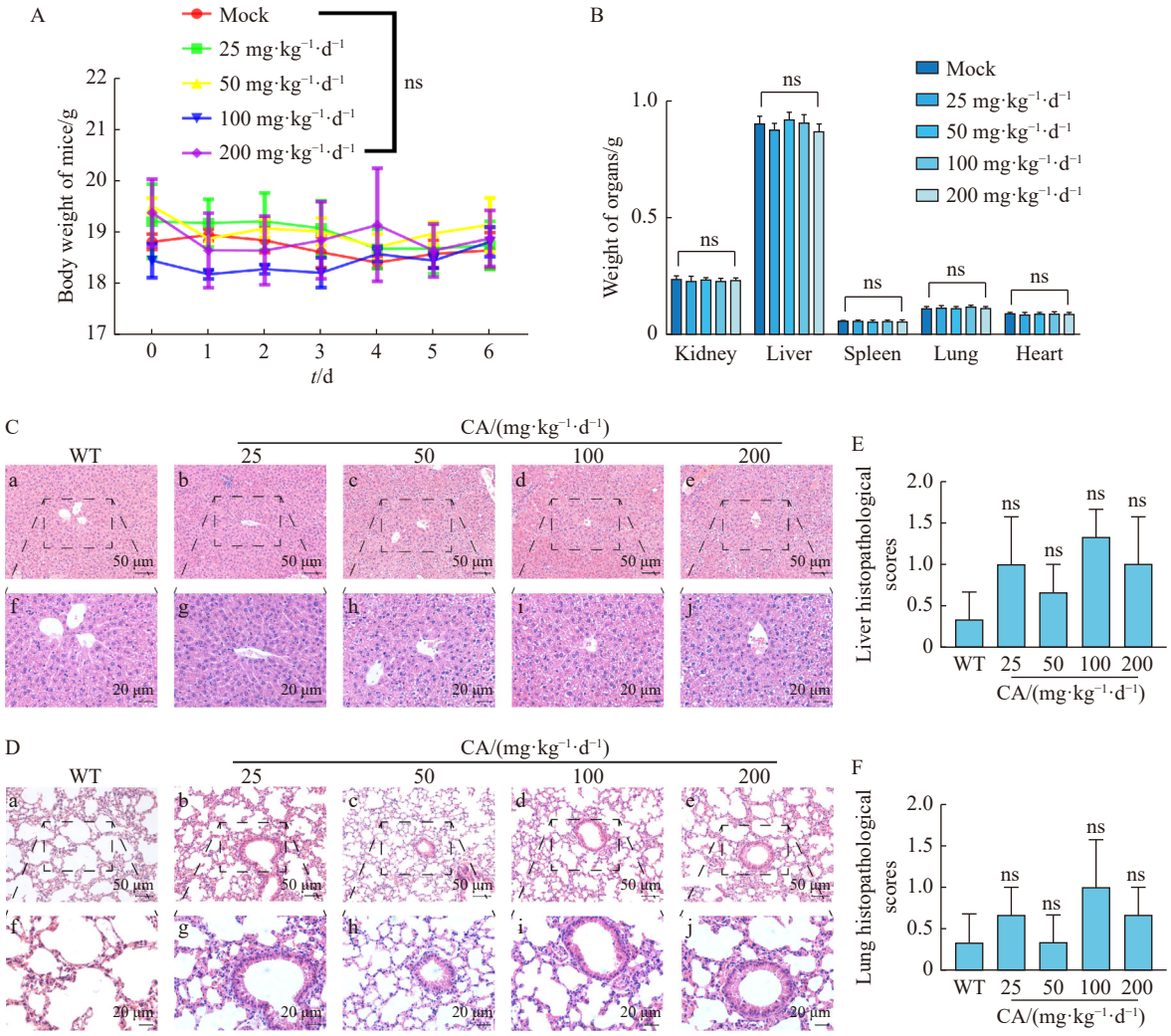

Fig. 3 Effects of different concentrations of CA on C57BL/6 mice. (A) Effects of continuous intragastric administration of different concentrations of CA (25–200 mg·kg^{-1}·d^{-1}) on the body weight of mice for 6 d (n = 5). (B) Effects of different concentrations of CA (25–200 mg·kg^{-1}·d^{-1}) gavage on the heart, kidney, lung, liver, and spleen weights of mice (n = 5). (C–F) Representative images of hematoxylin-eosin staining with different concentrations of CA on lung and liver toxicity and their semi-quantitative histological scores (n = 5). Data are represented as mean ± SEM, ns = no significance (a–e scale bar = 50 μm, f–j scale bar = 20 μm.

products [36]. Given Carrimycin's established antibiotic function, it is hypothesized that CA treatment could modulate the intestinal microflora in septic mice. To investigate this, we conducted 16S rRNA next-generation sequencing to analyze changes in intestinal microflora following CA treatment in septic mice. Our objective was to elucidate the relationship between CA's therapeutic effect (administered at 100 mg·kg^{-1}, three times *via* gavage) and alterations in the intestinal microflora of CLP-induced septic mice. We examined the gut microbiota across four different groups: Mock (control), CA, CLP (sepsis model), and CLP + CA (sepsis model treated with CA). The sequencing data revealed that the Shannon index curves of each group plateaued, indicating that the sequencing data had reached saturation; in other words, the diversity of features no longer increased with further sequencing (Fig. 6A). This observation enhances the credibility of the sequencing results. Venn diagrams were used to illustrate the number of operational taxonomic units (OTUs) common to or unique among the groups. Notably, the CLP + CA group exhibited a higher number of unique OTUs (46) compared with the Mock (5 OTUs), CA (3 OTUs), and CLP (5 OTUs) groups (Fig. 6B). Furthermore, a 3D principal coordinates analysis (PCoA) map was generated to display the differences in alpha diversity of microbial flora among the groups. The spatial separation between the groups in the PCoA plot reflected the variance in species diversity, suggesting distinct compositional structures in their microbial communities (Figs. 6C and S8A–8C). These findings indicate that CA treatment in CLP-induced septic mice leads to significant changes in the gut microbiota. This suggests a possible link between the therapeutic effects of CA and alterations in intestinal flora, providing a new perspective on the

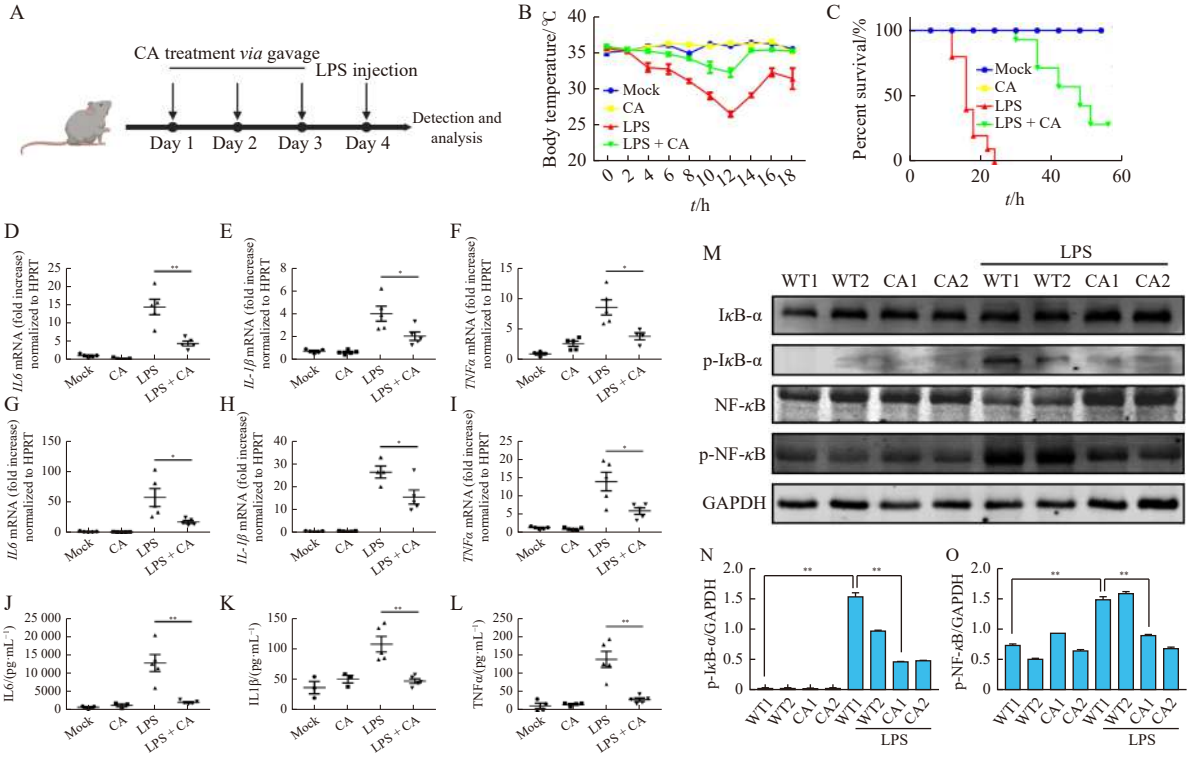

Fig. 4 Carrimycin treats LPS-induced inflammation in mice. (A) Mice treatment protocol. (B) Body temperature (n = 10). (C) Survival rate (n = 10). (D–F) Change in the expression of *IL-6*, *IL-1β*, and *TNF-α* mRNAs in the liver tissue (n = 5). (G–I) Change in the expression of *IL-6*, *IL-1β*, and *TNF-α* mRNAs in the lung tissue (n = 5). (J–L) Change in the level of IL-6, IL-1β, and TNF-α in the serum of mice (n = 5). (M–O) Western blotting assay shows the effect of CA on the NF-κB signaling pathway proteins in the lungs of LPS-induced inflammatory mice. The dosage of LPS was 15 mg·kg^{-1}. Data are represented as mean ± SEM, n = 5. $^{*}P < 0.05$, $^{**}P < 0.01$.

mechanisms by which CA may exert its beneficial effects in the treatment of sepsis.

The evaluation of alpha diversity in the microbial community, as indicated by the Accumulated Cyclone Energy (ACE), Chao1, Shannon, and Simpson indices, provides insights into the impact of CA on the gut microbiota in CLP-induced septic mice. The Shannon and Simpson indices were significantly lower in the CLP group compared with the Mock group, indicating reduced microbial diversity in the CLP-induced sepsis ($^{*}P < 0.05$, $^{***}P < 0.001$, Figs. 6D–6G). Notably, the alpha diversity, as reflected by all four indices (ACE, Chao1, Shannon, and Simpson), significantly increased in the CLP + CA group compared with the CLP group ($^{***}P < 0.001$, Figs. 6D–6G). Inflammatory bowel disease was associated with a reduction in alpha diversity of gut microbes [37]. Additionally, sepsis-related outcomes were markedly worsened by colitis [38]. This suggests that CA treatment enhances the alpha diversity of gut microbes in CLP mice.

To identify specific bacterial alterations induced by CA treatment and their implications for the disease progression in CLP-induced sepsis, we analyzed the top ten bacterial genera by relative abundance and generated heat maps (Figs. 6H–6I). The most enriched microbial species included *Escherichia_Shigella*, *Akkermansia*, *Bacteroides*, *unclassified_Muribaculaceae*, *Parabacteroides*, *Ligilactobacillus*, *Fusobacterium*, *[Clostridium]_innocuum_group*, *Klebsiella*, and *Alloprevotella* (Fig. S9).

Significantly, in CLP-induced sepsis, the proportion of *Escherichia_Shigella* dramatically increased (53.4%) compared with wild-type mice (5.5%, $P < 0.0001$). This aligns with other studies indicating Shigella as a major pathogen in CLP-induced septic mice [39]. *Shigella* is known to trigger caspase-11 activation in mice, leading to IL-1β expression and lethal septic shock [40]. Moreover, *Shigella* infection is associated with the development of sepsis [41, 42]. CA treatment notably reduced the prevalence of *Escherichia_Shigella* in CLP-induced mice (from 53.3% to 35.3%, $P < 0.0001$), which could be a crucial factor in CA's therapeutic efficacy in sepsis. Additionally, CA decreased the proportion of *Klebsiella* (from 0.7% to 0.4%, $P < 0.01$), a sepsis-associated opportunistic and drug-resistant bacterium [43, 44]. Conversely, the abundance of the probiotic Alloprevotella increased in CA-treated CLP mice (from 3.8% to 8.7%, $P < 0.0001$). *Alloprevotella* is known to facilitate the recovery of intestinal microbiota diversity [45], which is crucial for sepsis prevention and treatment.

In conclusion, these results suggest that CA influences the population and abundance of both probiotics and pathogenic microorganisms in the gut of septic mice, potentially

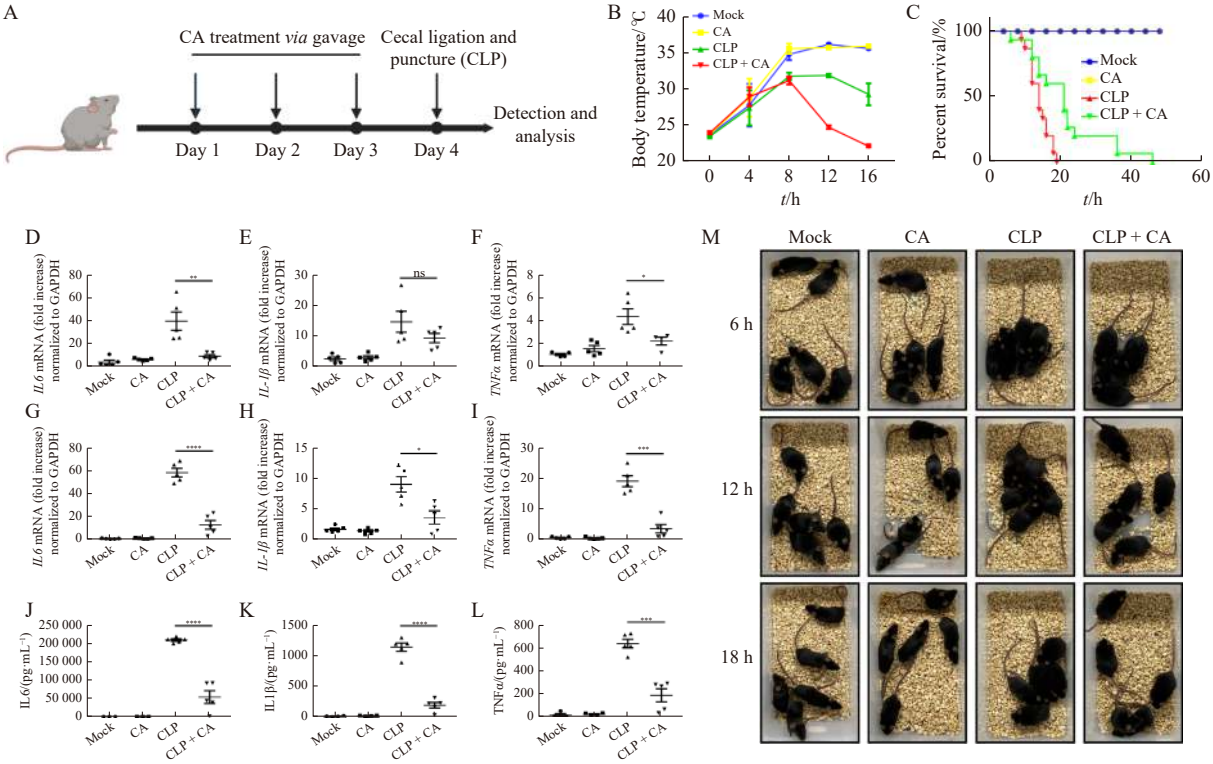

Fig. 5 The effect of CA on inflammation in CLP-induced mice. (A) Mice treatment protocol. (B) Body temperature (n = 5). (C) Survival rate (n = 15). (D–F) Effects of CA on mRNA expression of *IL-6*, *IL-1β*, and *TNF-α* in the liver of CLP mice (n = 5). (G–I) Effects of CA on mRNA expression of IL-6, IL-1β, and TNF-α in the lungs of CLP-induced mice (n = 5). (J–L) Effects of CA on IL-6, IL-1β, and TNF-α levels in the serum of CLP-induced mice (n = 5). (M) Observation of the effect of CA on CLP-induced mice from a behavioral perspective (n = 5). Data are represented as mean ± SEM. $^{*}P < 0.05$, $^{**}P < 0.01$, $^{***}P < 0.001$, $^{****}P < 0.0001$.

underpinning its therapeutic effect on CLP-induced sepsis. This highlights the significance of gut microbiota modulation in the treatment of sepsis and underscores the therapeutic potential of CA in this context.

Differential analysis and prediction of the effect of CA treatment on the gut microbiota in CLP-induced mice

To delve deeper into the specific bacterial alterations induced by CA treatment in CLP-induced sepsis and their impact on disease progression, we employed linear discriminant analysis of effect size (LEfSe). This high-dimensional statistical tool is adept at identifying significant differences in bacterial community dominance, providing a nuanced view of microbiota alterations. The LEfSe analysis was conducted to pinpoint statistical differences in the abundance of gut microbiota, ranging from the phylum to the species level (Fig. 7A) and to generate a corresponding cladogram (Fig. 7B), with a linear discriminant analysis (LDA) score cut-off greater than 4.0. The analysis confirmed that *Shigella* is a key bacterial type in CLP-induced sepsis in mice, aligning with expectations. Furthermore, the analysis revealed a significant enrichment of *Bacteroidota* (including the class *Bacteroidia*, the order *Bacteroidales*, the family *Prevotellaceae*, and the genera *Alloprevotella* and *Parabacteroides*) following CA treatment in CLP-induced mice. *Alloprevotella* is recognized as a probiotic, and research has indicated that *Parabacteroides*, also a probiotic, can regulate lung inflammation [46]. *Bacteroidota* and *Firmicutes* are known for producing short-chain fatty acids (SCFAs), such as butyric, propionic, and acetic acids. These SCFAs influence host metabolism by acting on G protein-coupled receptors expressed in enteroendocrine cells [47]. This implies that CA treatment in CLP-induced mice could exert its effects by modulating the abundance of specific gut microbiota, primarily *Bacteroidota*, and their metabolic products. In summary, these findings suggest that CA's therapeutic efficacy in CLP-induced sepsis may be partly mediated through the regulation of gut microbiota composition, particularly the promotion of beneficial bacterial groups like *Bacteroidota*, and the modulation of their metabolites. This microbiota-focused perspective offers a valuable understanding of CA's mechanism of action in sepsis treatment and underscores the importance of gut microbiota management in mitigating sepsis progression.

To further explore the influence of CA treatment on the functional activities of the gut microbiota in CLP-induced septic mice, we conducted a phylogenetic investigation of communities by reconstruction of unobserved states (PICRUSt). This approach maps 16S rRNA sequences to gene functions and pathways likely present in these bacterial populations, based on the Kyoto Encyclopedia of Genes and Genomes (KEGG) database, with a *P*-value threshold setting of 0.05. The PICRUSt analyses disclosed distinct metagenome functional content, identifying 26 core predicted categories

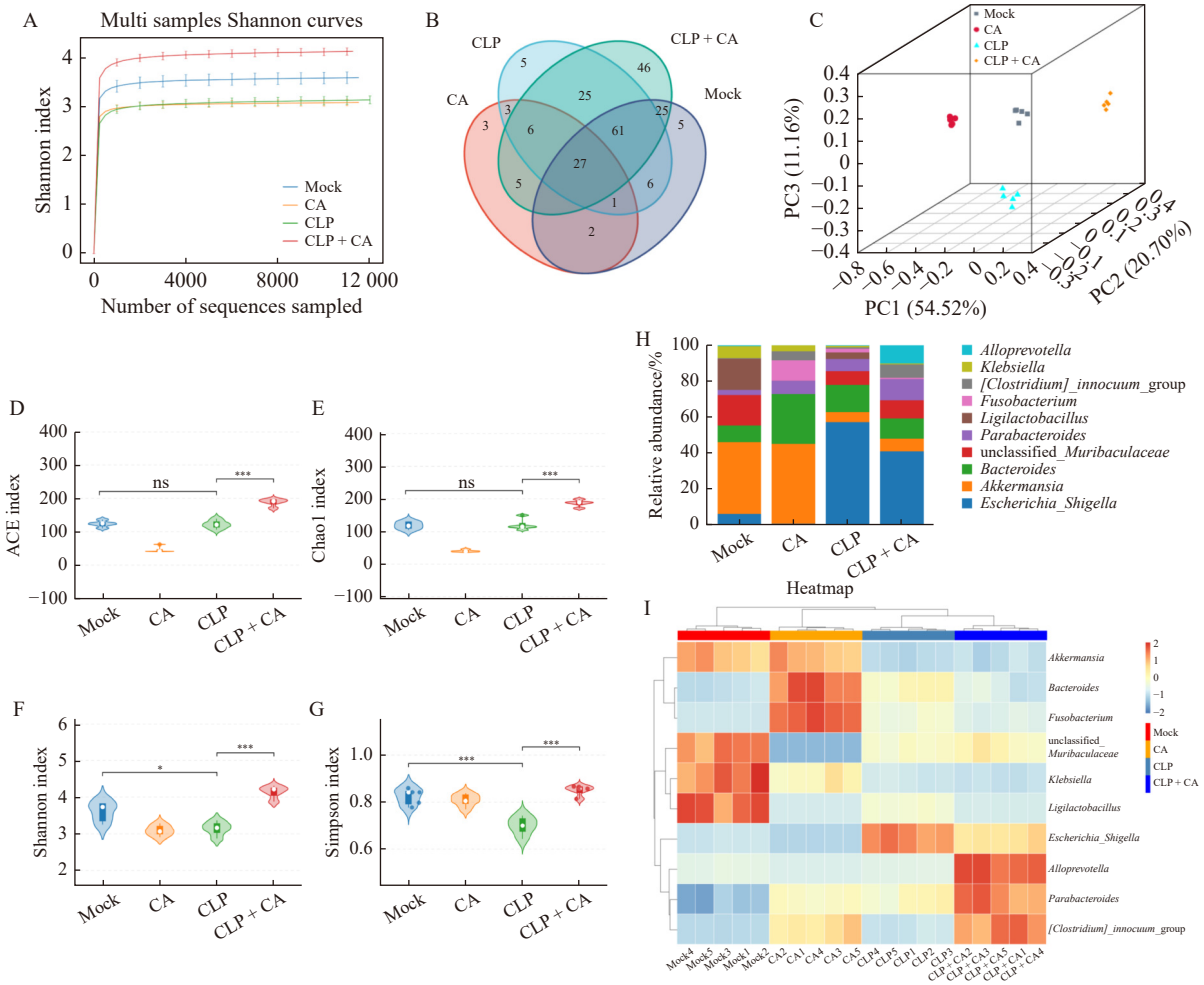

Fig. 6 Effects of CA on fecal microbiota in CLP-induced mice. (A) Shannon exponential curve for different groupings. (B) Venn plot showing the coincidence of features between different groups at the OTU level. (C) Binary Jaccard PCoA plot. (D–G) ACE index, Chao1 index, Shannon index, and Simpson index (n = 5). (H) Composition of the gut microbiota at the genus level. (I) Heatmap of gut microbes between different groups at the genus level. Data are represented as mean ± SEM. $^{*}P < 0.05$, $^{***}P < 0.001$.

(Fig. 7C). Analysis of KEGG pathway categories (level III) revealed significant enrichment in several metabolism-related pathways. These included "Biosynthesis of secondary metabolites" (increased from 7.11% in the CLP-induced group to 7.29% in the CLP-induced + CA-treated group, $P < 0.0001$), "Biosynthesis of amino acids" (from 3.33% to 3.71%, $P < 0.0001$), "Purine metabolism" (from 1.94% to 1.97%, $P < 0.01$), and "Glycolysis/Gluconeogenesis" (from 1.09% to 1.17%, $P < 0.0001$). Significantly, CA treatment upregulated these metabolic pathways in the gut microbiota of CLP-induced mice. SCFAs, primarily acetate, propionate, and butyrate, are mainly produced by the anaerobic fermentation of gut microbes [48]and were found to be upregulated by CA treatment. SCFA deficiency has been linked to inflammatory diseases, such as inflammatory bowel disease [49] and psoriatic arthritis [50]. The observed increase in SCFA content may correlate with the alleviation of inflammation in CLP-induced mice by CA treatment. Additionally, CA treatment significantly upregulated the "Biosynthesis of antibiotics" pathway (from 5.26% in the CLP-induced group to 5.43% in the CLP-induced + CA-treated group, $P < 0.0001$), which could further enhance the intestinal microbial environment in CLP-induced mice.

In summary, CA treatment not only altered the composition of the gut microbiota —marked by a decrease in the pathogenic bacterium *Shigella* and an increase in the probiotic *Bacteroidota*—but also affected the secretion of metabolites, particularly increasing the expression of SCFAs, by modulating the metabolic pathways of the gut microbiota. These findings suggest that CA treatment effectively modulates the gut microbial environment, thereby offering a potential therapeutic approach for treating CLP-induced sepsis in mice.

Carrimycin performs better than aspirin (ASP)/TIENAM in inhibiting LPS-induced inflammation in vivo

The study's comparison of the therapeutic effects of CA and ASP in the treatment of LPS-induced sepsis in mice provides critical insights into their relative anti-inflammatory

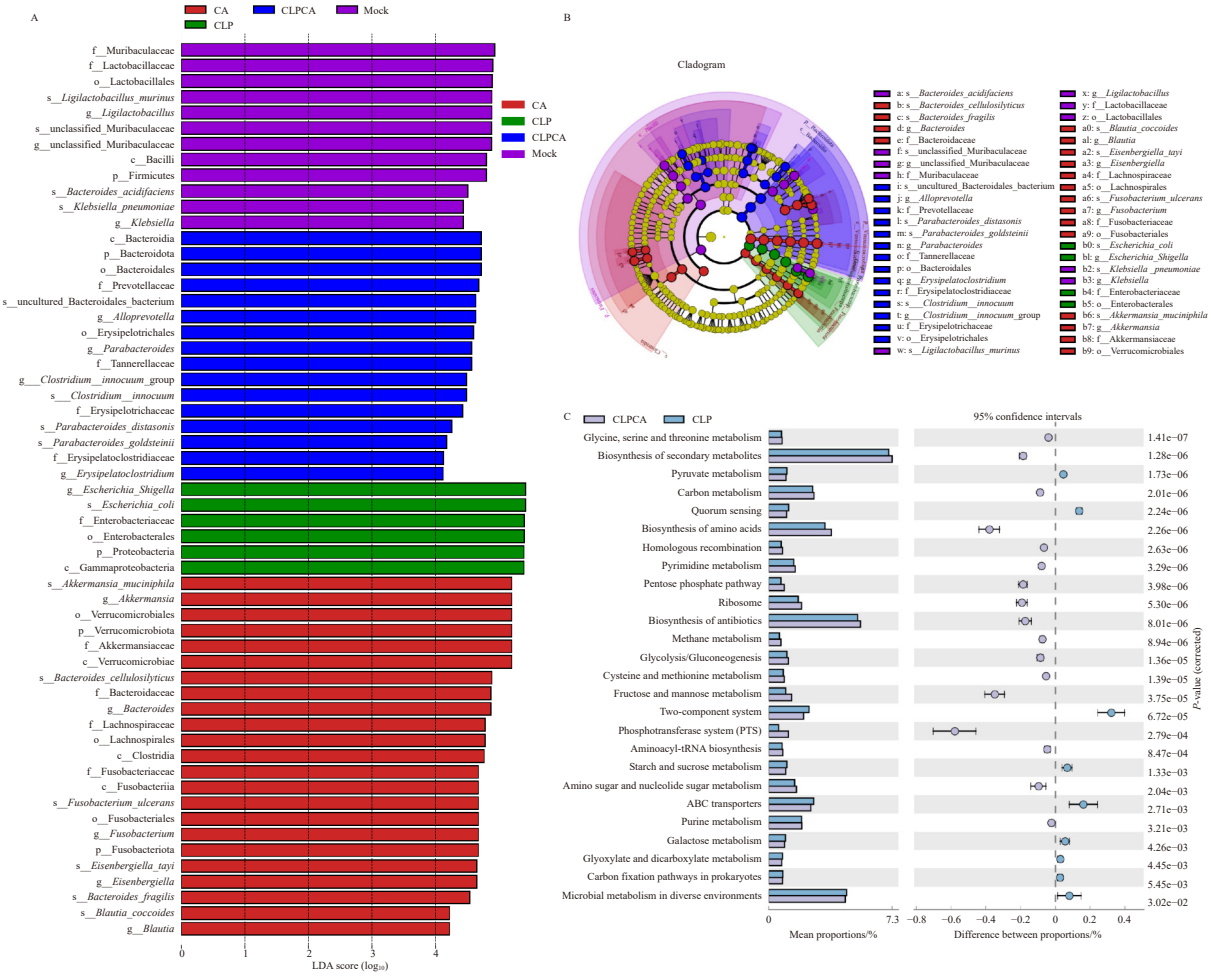

Fig. 7 Differential analysis and gene function prediction of gut microbial components between groups. (A) LEfSe analysis of gut microbiota (LDA score greater than 4.0). (B) Cladogram generated from LEfSe analysis. (C) The difference between CLP-induced and CLP-induced + CA-treated groups using PICRUSt functional gene prediction for gut microbiota (database selection: KEGG, *P* value threshold setting: 0.05).

capabilities. ASP, a classic anti-inflammatory agent, has been recommended for sepsis treatment [51] and is known to inhibit LPS-induced activation of the NF-κB pathway [52, 53]. Therefore, we compared the therapeutic effect of CA and ASP in the treatment of LPS-induced sepsis in mice.

In our analysis, both CA and ASP were administered at the same dosage (100 mg·kg^{-1}). The findings demonstrated that CA more effectively inhibited the mRNA expression of IL-6 in the lung tissue of LPS-induced mice than ASP (Figs. 8A–8C). This superior efficacy of CA was also evident in serum inflammatory factor levels (IL-6 and TNF-α) (Figs. 8D–8F), indicating that CA's anti-inflammatory potential surpasses that of ASP *in vivo* in response to LPS-induced inflammation.

Additionally, the study compared CA with TIENAM (imipenem/cilastatin), an NMPA-approved broad-spectrum antibiotic effective in treating bacterial pneumonia [54, 55]. The results showed that CA treatment significantly inhibited the LPS-induced mRNA expression of IL-6 and IL-1β *in vitro* more effectively than TIENAM treatment (Figs. S10A–10C). Moreover, *in vivo*, CA was more efficacious than TIENAM in reducing the mRNA expression of IL-6 and TNF-α in response to LPS-induced sepsis (Figs. S10D–10I). In conclusion, these results highlight CA's potent anti-inflammatory effects compared with both ASP and TIENAM. Its superior efficacy in inhibiting key pro-inflammatory cytokines in both *in vitro* and *in vivo* models of LPS-induced sepsis positions CA as a potentially more effective therapeutic agent in the management of sepsis.

Discussion

The timely administration of antibiotics during the early stages of sepsis is crucial for reducing the disease burden [14], with the management of inflammatory disorders being a focal point in sepsis treatment. While body fluid purification [10] and multiple cytokine blockers [56] are utilized in sepsis therapy, the complexity of pathogenic factors often limits the effectiveness of monotherapies. Current International Guidelines for the Management of Sepsis and Septic Shock primarily recommend macrolides as anti-resistant bacterial

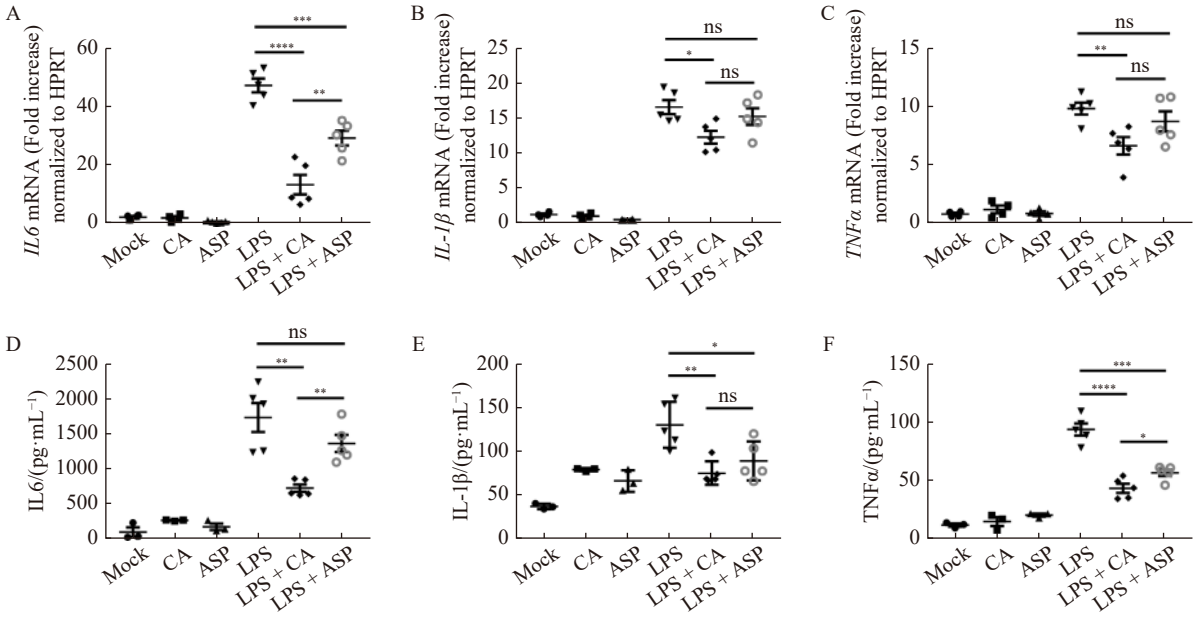

Fig. 8 Carrimycin performs better than ASP in inhibiting LPS-induced inflammation in mice. (A–C) The effect of CA and ASP on inhibiting the mRNA expression of *IL-6*, *IL-1β*, and *TNF-α* in mice lung tissue (n = 5). (D–F) The effect of CA and ASP in reducing IL-6, IL-1β, and TNF-α levels in the mice serum (n = 5). (The doses of CA and ASP were both 100 mg·kg^{-1}, administered three times, in which CA was administered by gavage and ASP was injected intraperitoneally. Data are represented as mean ± SEM. $^{*}P < 0.05$, $^{**}P < 0.01$, $^{***}P < 0.001$, $^{****}P < 0.0001$.

drugs in the early stages of sepsis, often overlooking their potential immunomodulatory functions [57-59]. CA, a newer macrolide antibiotic, has been endorsed by the NMPA for its antibacterial and anti-inflammatory efficacy, along with its safety profile, positioning it as a promising candidate in sepsis treatment.

This study demonstrated that CA effectively inhibits inflammation induced by LPS and CLP, highlighting its significant role in sepsis therapy. CA not only suppressed the inflammatory response induced by LPS in macrophage RAW264.7 and THP1 cells but also increased survival rates by inhibiting the inflammatory surge in LPS- and CLP-induced mice *in vivo*. Additionally, CA markedly improved thermoregulation in LPS- and CLP-induced septic mice, an important factor in managing sepsis. Crucially, CA decreased the expression of pro-inflammatory cytokines IL-6, IL-1β, and TNF-α in the peripheral blood, lungs, and liver of LPS- and CLP-induced septic mice. This indicates that CA treatment alleviates systemic inflammation and offers protective effects on the liver and lungs *in vivo*. Histopathological analysis using hematoxylin-eosin staining further corroborated CA's protective impact on lung and liver tissues in septic mice. Moreover, CA modified the gut microbiota's abundance and diversity, reducing the pathogen *Shigella* and increasing the proportion of the probiotic *Alloprevotella*. Furthermore, CA influences the metabolic pathways of intestinal microbes, notably enhancing the metabolic pathways of SCFAs, which are beneficial in mitigating bodily inflammation. In summary, these findings provide compelling evidence of CA's protective effects against sepsis-induced inflammatory disorders. By modulating both the immune response and the gut microbiota, CA emerges as a multifaceted therapeutic agent, offering a valuable addition to the current sepsis treatment paradigm.

The complexity of sepsis lies in its multifaceted pathogenesis, involving an initial inflammatory response triggered by pathogen invasion [60] and subsequent immunosuppression due to sustained inflammation [61]. During the early stages of sepsis, the activation of PRRs, including TLRs, RIG-I-like receptors, NOD-like receptors, and C-type lectin receptors, initiates an intracellular signaling cascade, leading to inflammation. A critical aspect of this response is the activation of the NF-*κ*B signaling pathway, primarily through LPS-induced TLR4 activation, which is responsible for the early inflammatory burst in sepsis. Controlling this pathway in the early stages is crucial for managing the progression of the disease. In this study, we discovered that CA modulates the NF-*κ*B signaling pathway, including the regulation of phosphorylated I*κ*B-α (p-I*κ*B-α) and NF-*κ*B (p-NF-*κ*B) induced by LPS, both *in vivo* and *in vitro*. This finding suggests that CA ameliorates sepsis by intervening in key inflammatory signaling pathways.

Another critical factor in the development of sepsis is the alteration in immune cell phenotype. In early sepsis, immune cells, particularly macrophages and natural killer (NK) cells, tend towards inflammatory activation. These cells can activate the TNF pathway in response to pathogen invasion, which in turn activates the immune response, including the NF-*κ*B pathway, thereby inducing inflammation through a cascade reaction [62]. Previous studies have indicated that depletion of Natural killer (NK) cells in sepsis models can reduce systemic inflammatory responses and hypothermia, enhance micro-

bial clearance, restore acid-base balance, and improve survival [63, 64]. However, the specific impact of CA on the expression and function of immune cells in sepsis remains to be further elucidated. More comprehensive data are needed to fully understand CA's effects on the immune cell dynamics during sepsis. Understanding these effects is crucial for developing more effective treatments and interventions for this complex and often deadly condition.

The gut microbiota is integral to maintaining gut barrier function and regulating immune cell function [65], playing a pivotal role in the progression of sepsis. As an established antibacterial drug, CA potentially influences the composition of the intestinal microflora, a relationship that necessitates further exploration. In this study, we observed that CA treatment effectively modified the gut microbial environment towards reducing inflammation. This was evidenced by the reduction of the pathogen *Shigella* and the increase of the probiotic *Alloprevotella*, along with an enhancement of the SCFA metabolic pathway. These changes collectively contributed to mitigating the development of sepsis, underscoring CA's potent regulatory function on gut microbiota in septic mice.

In summary, CA demonstrated effective inhibition of inflammation both *in vitro* and *in vivo*. CA therapy curtailed the expression and release of pro-inflammatory cytokines (IL-6, IL-1β, and TNF-α) and impeded the activation of the NF-κB pathway triggered by LPS. Furthermore, CA showed a remarkable therapeutic effect in mouse models of both LPS- and CLP-induced sepsis. It decelerated the progression of inflammation and exerted a protective effect on the lungs and liver *in vivo*. Additionally, CA played a critical role in enhancing the diversity and regulating the metabolic pathways of gut microbiota, particularly by augmenting the metabolic pathway of SCFA, in septic mice. These findings indicate that CA possesses significant therapeutic potential for treating inflammation development in sepsis, presenting a promising avenue for future clinical applications in sepsis management.

Supplementary Information

Supplementary data to this article can be obtained by sending E-mail to the corresponding authors.

References

[1] Singer M, Deutschman CS, Seymour CW, *et al*. The third international consensus definitions for sepsis and septic shock (Sepsis-3) [J]. *JAMA*, 2016, **315**(8): 801-810.

[2] Fröhlich E. Structure and function of blood-tissue barriers [J]. *Dtsch Med Wochenschr (1946)*, 2002, **127**(49): 2629-2634.

[3] Yende S, Linde-Zwirble W, Mayr F, *et al*. Risk of cardiovascular events in survivors of severe sepsis [J]. *Am J Respir Crit Care Med*, 2014, **189**(9): 1065-1074.

[4] Silasi-Mansat R, Zhu H, Popescu NI, *et al*. Complement inhibition decreases the procoagulant response and confers organ protection in a baboon model of *Escherichia coli* sepsis [J]. *Blood*, 2010, **116**(6): 1002-1010.

[5] Nieman MT. Protease-activated receptors in hemostasis [J]. *Blood*, 2016, **128**(2): 169-177.

[6] Opal S, van der Poll T. Endothelial barrier dysfunction in septic shock [J]. *J Intern Med*, 2015, **277**(3): 277-293.

[7] Hotchkiss RS, Monneret G, Payen D. Sepsis-induced immunosuppression: from cellular dysfunctions to immunotherapy [J]. *Nat Rev Immunol*, 2013, **13**(12): 862-874.

[8] Pastille E, Didovic S, Brauckmann D, *et al*. Modulation of dendritic cell differentiation in the bone marrow mediates sustained immunosuppression after polymicrobial sepsis [J]. *J Immunol*, 2011, **186**(2): 977-986.

[9] van der Poll T, Opal SM. Host–pathogen interactions in sepsis [J]. *Lancet Infect Dis*, 2008, **8**(1): 32-43.

[10] Kang JH, Super M, Yung CW, *et al*. An extracorporeal blood-cleansing device for sepsis therapy [J]. *Nat Med*, 2014, **20**(10): 1211-1216.

[11] Perner A, Gordon AC, De Backer D, *et al*. Sepsis: frontiers in diagnosis, resuscitation and antibiotic therapy [J]. *Intensive Care Med*, 2016, **42**(12): 1958-1969.

[12] Brown RM, Semler MW. Fluid management in sepsis [J]. *J Intensive Care Med*, 2019, **34**(5): 364-373.

[13] Leentjens J, Kox M, van der Hoeven JG, *et al*. Immunotherapy for the adjunctive treatment of sepsis: from immunosuppression to immunostimulation. Time for a paradigm change? [J]. *Am J Respir Crit Care Med*, 2013, **187**(12): 1287-1293.

[14] Ferrer R, Martin-Loeches I, Phillips G, *et al*. Empiric antibiotic treatment reduces mortality in severe sepsis and septic shock from the first hour: results from a guideline-based performance improvement program [J]. *Crit Care Med*, 2014, **42**(8): 1749-1755.

[15] Roberts JA, Abdul-Aziz MH, Davis JS, *et al*. Continuous versus intermittent β-lactam infusion in severe sepsis. A meta-analysis of individual patient data from randomized trials [J]. *Am J Respir Crit Care Med*, 2016, **194**(6): 681-691.

[16] Abdul-Aziz MH, Sulaiman H, Mat-Nor M-B, *et al*. β-Lactam infusion in severe sepsis (BLISS): a prospective, two-centre, open-labelled randomised controlled trial of continuous versus intermittent β-lactam infusion in critically ill patients with severe sepsis [J]. *Intensive Care Med*, 2016, **42**(10): 1535-1545.

[17] Shang GD, Dai JL, Wang YG. Construction and physiological studies on a stable bioengineered strain of shengjimycin [J]. *J Antibiot (Tokyo)*, 2001, **54**(1): 66-73.

[18] Shi XG, Sun YM, Zhang YF, *et al*. Tissue distribution of bitespiramycin and spiramycin in rats [J]. *Acta Pharmacol Sin*, 2004, **25**(11): 1396-1401.

[19] Shi XG, Fawcett JP, Chen XY, *et al*. Structural identification of bitespiramycin metabolites in rat: a single oral dose study [J]. *Xenobiotica*, 2005, **35**(4): 343-358.

[20] Zhong DF, Shi XG, Sun L, *et al*. Determination of three major components of bitespiramycin and their major active metabolites in rat plasma by liquid chromatography-ion trap mass spectrometry [J]. *J Chromatogr B Analyt Technol Biomed Life Sci*, 2003, **791**(1-2): 45-53.

[21] He WQ, Yang CP, Zhao XF, *et al*. Antimicrobial activity of bitespiramycin, a new genetically engineered macrolide [J]. *Bioorg Med Chem Lett*, 2017, **27**(19): 4576-4577.

[22] Morgan AM, Roden RC, Matson SC, *et al*. Severe sepsis and acute myocardial dysfunction in an adolescent with *Chlamydia trachomatis* pelvic inflammatory disease: a case report [J]. *J Pediatr Adolesc Gynecol*, 2018, **31**(2): 143-145.

[23] Rodríguez RB, Etayo BZ, Aguar RB, *et al*. Community-acquired pneumonia, acute respiratory distress syndrome, and severe sepsis due to *Chlamydia pneumoniae* [J]. *Rev Clin Esp*, 2002, **202**(11): 623.

[24] Pinna GS, Skevaki CL, Kafetzis DA. The significance of *Ureaplasma urealyticum* as a pathogenic agent in the paediatric population [J]. *Curr Opin Infect Dis*, 2006, **19**(3): 283-289.

[25] Yan HY, Sun J, Wang K, *et al*. Repurposing carrimycin as an antiviral agent against human coronaviruses, including the currently pandemic SARS-CoV-2 [J]. *Acta Pharm Sin B*, 2021, **11**(9): 2850-2858.

[26] Liang SY, Zhao TC, Zhou ZH, *et al*. Anti-tumor effect of carrimycin on oral squamous cell carcinoma cells *in vitro* and *in vivo* [J]. *Transl Oncol*, 2021, **14**(6): 101074.

[27] Jin Y, Zuo HX, Li MY, *et al*. Anti-tumor effects of carrimycin and monomeric isovalerylspiramycin I on hepatocellular carcinoma *in vitro* and *in vivo* [J]. *Front Pharmacol*, 2021, **12**: 774231.
[28] Cui J, Zhou J, He W, *et al*. Targeting selenoprotein H in the nucleolus suppresses tumors and metastases by isovalerylspiramycin I [J]. *J Exp Clin Cancer Res*, 2022, **41**(1): 126.
[29] Behal ML, Nguyen JL, Li X, *et al*. Azithromycin and major adverse kidney events in critically Ill patients with sepsis-associated acute kidney injury [J]. *Shock*, 2022, **57**(4): 479-485.
[30] Rittirsch D, Huber-Lang MS, Flierl MA, *et al*. Immunodesign of experimental sepsis by cecal ligation and puncture [J]. *Nat Protoc*, 2009, **4**(1): 31-36.
[31] Bosmann M, Ward PA. The inflammatory response in sepsis [J]. *Trends Immunol*, 2013, **34**(3): 129-136.
[32] Pham CG, Bubici C, Zazzeroni F, *et al*. Ferritin heavy chain upregulation by NF-κB inhibits TNFα-induced apoptosis by suppressing reactive oxygen species [J]. *Cell*, 2004, **119**(4): 529-542.
[33] Lelubre C, Vincent JL. Mechanisms and treatment of organ failure in sepsis [J]. *Nat Rev Nephrol*, 2018, **14**(7): 417-427.
[34] Park I, Kim M, Choe K, *et al*. Neutrophils disturb pulmonary microcirculation in sepsis-induced acute lung injury [J]. *Eur Respir J*, 2019, **53**(3): 1800786.
[35] Dejager L, Pinheiro I, Dejonckheere E, *et al*. Cecal ligation and puncture: the gold standard model for polymicrobial sepsis? [J]. *Trends Microbiol*, 2011, **19**(4): 198-208.
[36] Adelman MW, Woodworth MH, Langelier C, *et al*. The gut microbiome's role in the development, maintenance, and outcomes of sepsis [J]. *Crit Care*, 2020, **24**(1): 278.
[37] Duvallet C, Gibbons SM, Gurry T, *et al*. Meta-analysis of gut microbiome studies identifies disease-specific and shared responses [J]. *Nat Commun*, 2017, **8**(1): 1784.
[38] Colbert JF, Schmidt EP, Faubel S, *et al*. Severe sepsis outcomes among hospitalizations with inflammatory bowel disease [J]. *Shock*, 2017, **47**(2): 128-131.
[39] Liang H, Song H, Zhang X, *et al*. Metformin attenuated sepsis-related liver injury by modulating gut microbiota [J]. *Emerg Microbes Infect*, 2022, **11**(1): 815-828.
[40] Kayagaki N, Stowe IB, Lee BL, *et al*. Caspase-11 cleaves gasdermin D for non-canonical inflammasome signalling [J]. *Nature*, 2015, **526**(7575): 666-671.
[41] Kayagaki N, Wong MT, Stowe IB, *et al*. Noncanonical inflammasome activation by intracellular LPS independent of TLR4 [J]. *Science*, 2013, **341**(6151): 1246-1249.
[42] Nayyar C, Thakur P, Tak V, *et al*. *Shigella sonnei* sepsis in an infant: a case report [J]. *J Clin Diagn Res*, 2017, **11**(5): DD01-DD02.
[43] Li SX, Yu SF, Peng MF, *et al*. Clinical features and development of sepsis in *Klebsiella pneumoniae* infected liver abscess patients: a retrospective analysis of 135 cases [J]. *BMC Infect Dis*, 2021, **21**(1): 597.
[44] Dong N, Yang XM, Chan EW, *et al*. *Klebsiella* species: Taxonomy, hypervirulence and multidrug resistance [J]. *EBioMedicine*, 2022, **79**: 103998.
[45] Wang JK, He YT, Yu DQ, *et al*. Perilla oil regulates intestinal microbiota and alleviates insulin resistance through the PI3K/AKT signaling pathway in type-2 diabetic KKAy mice [J]. *Food Chem Toxicol*, 2020, **35**: 110965.
[46] Lai HC, Lin TL, Chen TW, *et al*. Gut microbiota modulates COPD pathogenesis: role of anti-inflammatory *Parabacteroides goldsteinii* lipopolysaccharide [J]. *Gut*, 2022, **71**(2): 309-321.
[47] Fan Y, Pedersen O. Gut microbiota in human metabolic health and disease [J]. *Nat Rev Microbiol*, 2021, **19**(1): 55-71.
[48] Pascale A, Marchesi N, Marelli C, *et al*. Microbiota and metabolic diseases [J]. *Endocrine*, 2018, **61**(3): 357-371.
[49] Wang W, Chen L, Zhou R, *et al*. Increased proportions of *Bifidobacterium* and the *Lactobacillus* group and loss of butyrate-producing bacteria in inflammatory bowel disease [J]. *J Clin Microbiol*, 2014, **52**(2): 398-406.
[50] Scher JU, Ubeda C, Artacho A, *et al*. Decreased bacterial diversity characterizes the altered gut microbiota in patients with psoriatic arthritis, resembling dysbiosis in inflammatory bowel disease [J]. *Arthritis Rheumatol*, 2015, **67**(1): 128-139.
[51] Das UN. Combination of aspirin with essential fatty acids is superior to aspirin alone to prevent or ameliorate sepsis or ARDS [J]. *Lipids Health Dis*, 2016, **15**(1): 206.
[52] Liu Y, Fang S, Li X, *et al*. Aspirin inhibits LPS-induced macrophage activation *via* the NF-κB pathway [J]. *Sci Rep*, 2017, **7**(1): 11549.
[53] Jiang R, Wei L, Zhu M, *et al*. Aspirin inhibits LPS-induced expression of PI3K/Akt, ERK, NF-κB, CX3CL1, and MMPs in human bronchial epithelial cells [J]. *Inflammation*, 2016, **39**(2): 643-650.
[54] Xie XD, Pang B. Clinical curative effect of Tienam combined with bronohoalveolar lavage on severe pneumonia and its influences on serum inflammatory indexes [J]. *J North Sichuan Med College*, 2021, **36**(11): 1501-1507.
[55] Wang F, Zhou QY, Lu T. Imipenem cilastatin sodium/meropenem in the treatment of patients with early lung cancer complicated severe pulmonary infection [J]. *Chin J Clin Res*, 2022, **35**(9): 1305-1309.
[56] Beltrán-García J, Osca-Verdegal R, Pallardó FV, *et al*. Sepsis and coronavirus disease 2019: common features and anti-inflammatory therapeutic approaches [J]. *Crit Care Med*, 2020, **48**(12): 1841-1844.
[57] Yoshioka D, Kajiwara C, Ishii Y, *et al*. Efficacy of β-lactam-plus-macrolide combination therapy in a mouse model of lethal pneumococcal pneumonia [J]. *Antimicrob Agents Chemother*, 2016, **60**(10): 6146-6154.
[58] Amado-Rodríguez L, González-López A, López-Alonso I, *et al*. Anti-inflammatory effects of clarithromycin in ventilator-induced lung injury [J]. *Respir Res*, 2013, **14**(1): 1-9.
[59] Patel A, Joseph J, Periasamy H, *et al*. Azithromycin in combination with ceftriaxone reduces systemic inflammation and provides survival benefit in a murine model of polymicrobial sepsis [J]. *Antimicrob Agents Chemother*, 2018, **62**(9): e00752-00718.
[60] Takeuchi O, Akira S. Pattern recognition receptors and inflammation [J]. *Cell*, 2010, **140**(6): 805-820.
[61] van der Poll T, van de Veerdonk FL, Scicluna BP, *et al*. The immunopathology of sepsis and potential therapeutic targets [J]. *Nat Rev Immunol*, 2017, **17**(7): 407-420.
[62] Jensen IJ, McGonagill PW, Butler NS, *et al*. NK cell–derived IL-10 supports host survival during sepsis [J]. *J Immunol*, 2021, **206**(6): 1171-1180.
[63] Christaki E, Diza E, Giamarellos-Bourboulis EJ, *et al*. NK and NKT cell depletion alters the outcome of experimental pneumococcal pneumonia: relationship with regulation of interferon-γ production [J]. *J Immunol Res*, 2015, **2015**: 532717.
[64] Greenberg AH. The origins of the NK cell, or a Canadian in King Ivan's court [J]. *Clin Invest Med*, 1994, **17**(6): 626-631.
[65] Haak BW, Wiersinga WJ. The role of the gut microbiota in sepsis [J]. *Lancet Gastroenterol Hepatol*, 2017, **2**(2): 135-143.

Cite this article as: LAI Junzhong, LIANG Jiadi, CHEN Kunsen, GUAN Biyun, CHEN Zhirong, CHEN Linqin, FAN Jiqiang, ZHANG Yong, LI Qiumei, SU Jingqian, CHEN Qi, LIN Jizhen. Carrimycin ameliorates lipopolysaccharide and cecal ligation and puncture-induced sepsis in mice [J]. *Chin J Nat Med*, 2024, **22**(3): 235-248.